Leveraging the effects of chloroquine on resistant malaria parasites for combination therapies

By: Ana M. Untaroiu [1]^, Maureen A. Carey [2]^, Jennifer L. Guler [3]*, & Jason A. Papin [1]*

Affiliations: Departments of [1] Biomedical Engineering, [2] Microbiology, Immunology, and Cancer Biology, and [3] Biology, University of Virginia, Charlottesville, VA, USA

^ Co-first authors

* Co-corresponding authors

Contact information:

Jennifer L. Guler (co-corresponding author): jlg5fw@virginia.edu

Jason A. Papin (co-corresponding author): papin@virginia.edu

Keywords:

Malaria, combination therapies, chloroquine, metabolic modeling

List of abbreviations:

CQ: chloroquine, DEG: differentially expressed gene, FBA: flux balance analysis, FC: fold change, FDR: false-discovery rate, MADE: Metabolic Adjustment for Differential Expression

Abstract

Malaria is a major global health problem, with the *Plasmodium falciparum* protozoan parasite causing the most severe form of the disease. Prevalence of drug-resistant *P. falciparum* highlights the need to understand the biology of resistance and to identify novel combination therapies that are effective against resistant parasites. Resistance has compromised the therapeutic use of many antimalarial drugs, including chloroquine, and limited our ability to treat malaria across the world. Fortunately, chloroquine resistance comes at a fitness cost to the parasite; this can be leveraged in developing combination therapies or to reinstate use of chloroquine. To understand biological changes induced by chloroquine treatment, we compared transcriptomics data from chloroquine-resistant parasites in the presence or absence of the drug. Using both linear models and a genome-scale metabolic network reconstruction of the parasite to interpret the expression data, we identified targetable pathways in resistant parasites. This study identified an increased importance of lipid synthesis, glutathione production/cycling, isoprenoids biosynthesis, and folate metabolism in response to chloroquine. We identified potential drug targets for chloroquine combination therapies. Significantly, our analysis suggests that the combination of chloroquine and sulfadoxine-pyrimethamine or fosmidomycin may be more effective against chloroquine-resistant parasites than either drug alone; further studies will explore the use of these drugs as chloroquine resistance blockers. Additional metabolic weaknesses were found in glutathione generation and lipid synthesis during chloroquine treatment. These processes could be targeted with novel inhibitors to reduce parasite growth and reduce the burden of malaria infections. Thus, we identified metabolic weaknesses of chloroquine-resistant parasites and propose targeted chloroquine combination therapies.

Background

There are approximately 3.2 billion people at risk of malaria infection worldwide and the malaria parasites cause half a million deaths annually (1). Given the lack of a broadly effective vaccine, antimalarial drugs and protection from mosquito bites are essential in the control of malaria (2). The most lethal species of the protozoan parasite that causes malaria, *Plasmodium falciparum*, has acquired resistance to every antimalarial drug on the market (3,4). Since the development of novel antimalarials is slow, there is a need for combination therapies to target resistant parasites.

First introduced in 1934, chloroquine was a front-line antimalarial until the late 1950s when its heavy usage led to emergence of resistant *P. falciparum* strains near the Cambodia-Thailand border (5). Chloroquine resistance has now been confirmed in over 40 countries, making resistance to this drug a global concern (5). The mechanism of action of chloroquine is well studied. In intraerythrocytic trophozoite parasites, the drug blocks detoxification of heme, a byproduct of hemoglobin degradation (6). During the asexual intraerythrocytic-stages, the parasite imports host cell hemoglobin into its food vacuole (7,8). Proteases in the food vacuole degrade hemoglobin into free amino acids which are utilized in various growth processes (9). Heme is released during hemoglobin digestion and is essential for parasite growth as a cofactor for cytochromes in the parasite's electron transport chain (10,11); however, elevated levels of intracellular heme can lead to cellular damage: oxidation of proteins, inhibition of proteases, and damage or lysis of membranes (12–14). Heme released from hemoglobin is detoxified through three known mechanisms: [1] polymerization into hemozoin crystals, [2] detoxification through interactions with hydrogen peroxide in the food vacuole, and [3] a glutathione-mediated degradation process in the cytoplasm (7,13,15,16). Chloroquine chemically binds to heme and the growing ends of hemozoin crystals, preventing crystallization-mediated heme detoxification (17,18).

Chloroquine-resistant parasites are able to export chloroquine (19), which reduces the accessibility of chloroquine to its heme and hemozoin targets (20,21). This resistance phenotype is mediated by mutations in the *P. falciparum* chloroquine resistance transporter (*pfcrt*) gene that results in the removal of drug from its functional site, the food vacuole (22,23). Numerous mutations are associated with chloroquine resistance, depending on the genetic background, and result in varying degrees of resistance (22,24–26). However, the substitution of lysine to threonine at position 76 in *pfcrt* is found in all *in vitro* chloroquine-resistant parasites (27,28).

Although chloroquine resistance is a well-studied case of antimalarial resistance, the mechanistic details remain poorly characterized. Studies on hemozoin formation estimate that only a third of heme released from hemoglobin is sequestered into hemozoin, suggesting a majority of heme is broken down through alternative, less well-characterized mechanisms, like peroxidative and glutathione degradation (16,29). Additional investigations are needed to understand the interplay between these mechanisms, which may become important in situations where resistant parasites are exposed to chloroquine. This situation is a greater possibility today, as some malaria endemic countries consider reintroducing chloroquine into their treatment regimens. Chloroquine resistance confers a fitness cost; thus, resistance alleles do not become fixed and decline in prevalence after chloroquine use is discontinued (30,31). As a result, clinical trials have confirmed that reintroduction of chloroquine is highly efficacious (32,33). Based on these findings, a reintroduction of chloroquine as a part of combination therapies may be an effective treatment strategy.

This study investigates the effects of chloroquine on chloroquine-resistant parasites to identify partner drugs that could be used in combination therapies to accelerate the reintroduction of chloroquine. We integrated the transcriptomics data from chloroquine-resistant parasites with or without chloroquine treatment (34) into a *P. falciparum* genome-scale metabolic network reconstruction to predict large-scale metabolic changes initiated by drug treatment, as we previously performed to study artemisinin resistance

(35). We identified shifts in metabolic flux and clinically available inhibitors that may partner well with chloroquine to target chloroquine resistant parasites.

Methods

Differential Gene Analysis: Expression data from *in vitro* K1 parasites untreated or treated with EC_{50} concentrations of chloroquine for 4hr and 24hrs were used to investigate the transcriptional effects of chloroquine treatment (normalized expression data obtained via GEO accession number: GSE31109) (34). Exposure for 4 and 24 hours were defined as short and long-term treatment, respectively. Probes with missing expression values were set equal to the lowest expression value across all replicates for that probe (35). Mean or median values across replicates were not used to replace missing expression values to avoid skewing the data with outliers. Genes with multiple probes were filtered from the data to ensure each gene corresponds to only one microarray probe. For repeating probes, only expression data from the probe with the largest variance across all replicates were retained. Means from repeating probes were not used to prevent averaging true signal with background noise. Probes with missing gene IDs were removed from the dataset.

The R package limma was used to conduct differential gene expression analysis **(Figure 1)**. Limma uses linear models to fit a data set and empirical Bayes statistical methods to determine variability and log-fold changes in gene expression (36). Significance values from this analysis (p-values) were modified using false discovery rate (FDR) correction in order to control for the parallel manner of comparing genes using limma, instead of testing genes in isolation. Differentially expressed genes were characterized as genes having a fold change (FC) greater than 2 or less than 0.5 and a FDR-adjusted p-value less than 0.05.

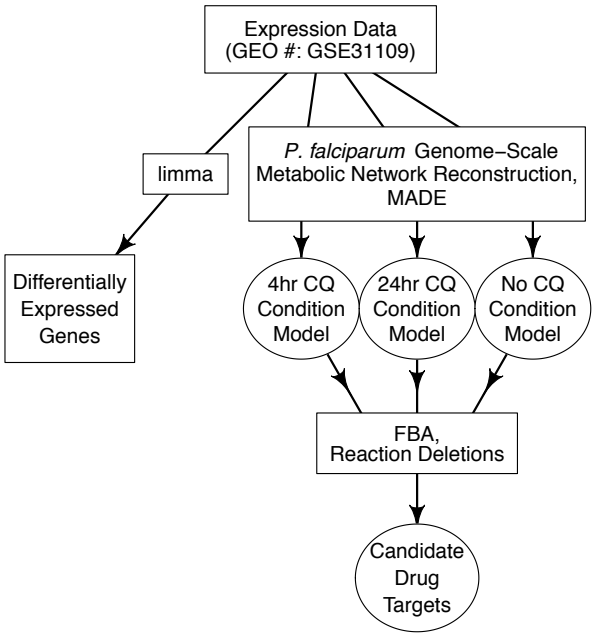

Figure 1: Overview of Computational Approach. The R package limma was used to find differentially expressed genes (left square). Metabolic Adjustment for Differential Expression (MADE) algorithm was used to produce the condition-specific models (right 3 circles). Flux balance analysis (FBA) and simulated reaction deletions predicted drug targets for chloroquine-treated parasites. CQ = Chloroquine.

Model Curation: Additional reactions were included into the *P. falciparum* model based on supporting experimental evidence (35). More specifically, hydrogen peroxide was incorporated as a byproduct of hemoglobin digestion based on studies of the chemical steps in hemoglobin breakdown (37). Reactions for heme degradation via glutathione and hydrogen peroxide were incorporated based on supporting literature (38,39). See **Supplemental Table 1** for modified reactions.

Condition-specific Model Generation: Condition-specific models were produced by integrating gene IDs with corresponding log FCs and FDR-adjusted p-values from the 4 and 24 hour treatment conditions into a curated version (see above) of the intraerythrocytic-stage *P. falciparum* genome-scale metabolic network reconstruction (35) (**Figure 1**). Data integration was conducted by using the Metabolic Adjustment for Differential Expression (MADE) algorithm; this algorithm accounts for the expression state of a gene with a weighted consideration of the statistical significance of the gene expression changes (40). Condition-specific models were generated for each condition (4hr chloroquine-treated, 24hr chloroquine-treated, and untreated) using varying growth thresholds (30 – 80%). This threshold represents the fraction of metabolic objective required for the output condition-specific model. We explored the effects of this threshold on condition-specific models to find minor differences in results. This paper reports common results across all models.

Reaction Essentiality Predictions and Flux Analysis: Essential reactions for each condition-specific model were generated by sequentially removing single reactions and testing the modified model for growth using flux balance analysis (41) (**Figure 1**). Reactions were delineated as essential when the removal of the reaction from the model resulted in a decrease of the growth rate by 60% or more compared to the untreated model. This growth rate threshold was chosen to avoid a too conservative definition of essentiality, but to also ensure a significant growth defect. Existing algorithms in the COBRA toolbox were used to calculate ranges of possible flux levels through reactions in the condition-specific models (42,43). Generation of condition-specific models, reaction essentiality, and flux analysis were conducted using MATLAB vR2014a, COBRA Toolbox v3.0, and Gurobi 6.5.2 solver.

Enrichment Analysis: The enrichment of metabolic subsystems among essential reactions were investigated. The purpose of this analysis is to determine whether a certain subsystem appears to a greater or lesser extent than expected by chance. Corresponding metabolic subsystems for genes and reactions were derived from the genome-scale metabolic model used in this study (35). We tested for enrichment of subsystems among essential genes with reference to the unconstrained model using a Fisher's exact test. Significant subsystems were defined as having a FDR-adjusted p-value less than 0.05. RStudio v3.3.0 was used for the differential gene and enrichment analysis.

Results

Resistant parasites respond to chloroquine pressure with moderate but statistically significant gene down-regulation. Since this analysis was not performed in the original study (34), differentially expressed genes (DEGs) were identified for both short and long-term treatment relative to untreated trophozoite expression. The majority of genes do not show a significant change in expression in response to chloroquine treatment (genes represented by points in black, **Figure 2**). Out of a total of 5,121 genes, there were 97 and 166 differentially expressed genes (DEGs) in short- and long-term treatment conditions, respectively (represented by points in red, **Figure 2**). In both conditions, more genes were significantly down-regulated than up-regulated in response to chloroquine treatment (95.9% for short-term and 83.1% for long-term treatment, fold change less than 0.5, **Suppl. Table 2**). Up-regulated genes showed very moderate over-expression (fold change between 2 and 2.5) and included one metabolic gene (**Suppl.**

Table 3). No evidence was found to suggest these DEGs are directly involved in chloroquine treatment or resistance.

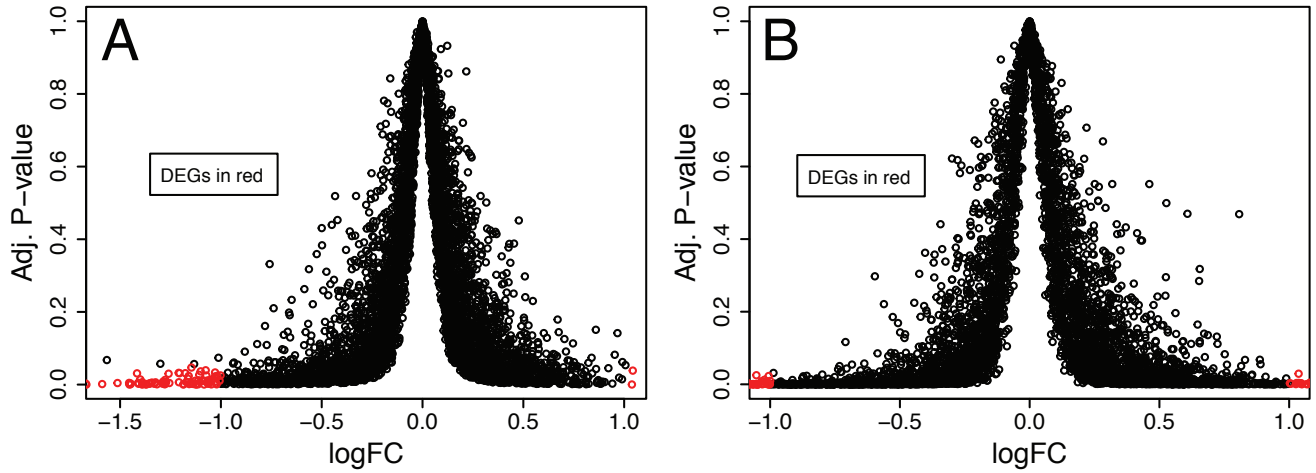

Figure 2: Resistant Parasites Respond to Drug by Downregulating Expression. FDR-adjusted p-values and fold changes (FC, reported as log values) for genes during (A) short-term treatment and (B) long-term treatment with chloroquine. Adjusted p-values represent the significance level of changes in expression. Fold change quantifies the variation in the gene expression relative to untreated resistant parasite expression. DEGs = differentially expressed genes.

Identifying metabolic weakness of chloroquine-treated resistant parasites using metabolic modeling. In order to understand the system-wide context for these gene expression changes, we integrated transcriptomics data into a genome-scale metabolic network reconstruction of intraerythrocytic-stage *P. falciparum* to generate three condition-specific models (untreated, short- and long-term chloroquine treatment). We then predicted reactions essential for parasite growth. One hundred and sixty-four metabolic reactions (out of 1197) are essential in all three models (**Figure 3A,** center); these reactions represent core metabolic pathways of the parasite.

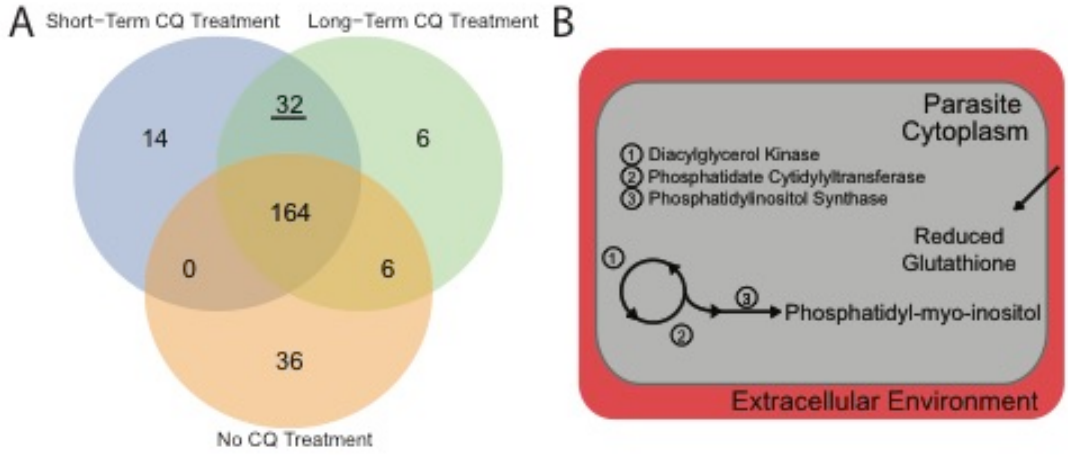

Figure 3. Chloroquine-treated parasites have new metabolic weaknesses. (**A**) Comparison of essential reactions in the three condition-specific models (one for each condition: short-term and long-term chloroquine treatment, as well as the untreated condition). (**B**) Illustration of common essentiality predictions (underlined in A) between the drug-treatment models, including inositol phosphate metabolism and glutathione import are represented. These enzymes could be targeted in these resistant parasites in combination with chloroquine; resultant combination

therapies would specifically target resistant parasites during chloroquine treatment, not wild-type parasites or single-drug treatment. Red region depicts the host red blood cell and grey is the parasite's cytoplasm.

Reactions that become essential during chloroquine treatment highlight weak points in the metabolic network and can be exploited as drug targets in chloroquine-resistant parasites. We found 210 and 208 essential metabolic reactions in short- and long-term treatment, respectively. Thirty-two were shared between the two conditions **(Suppl. Table 5, Figure 3**); fifteen of these are involved in phosphatidylethanolamine and phosphatidylserine metabolism, seven in phospholipid utilization, and one in the import of reduced glutathione (examples summarized in **Figure 3B**; **Suppl. Table 5**). When we performed subsystem enrichment on the essential reactions, the following subsystems were over-represented: phosphatidylethanolamine and phosphatidylserine metabolism (p-value = 4.84E-6), tRNA synthesis (p-value = 0.024), and phospholipid utilization (p-value = 0.037). Reactions involved in transport and lipid metabolism were under-represented in chloroquine treated models (p-value = 0.0061 and 2.51E-8, respectively).

Fourteen reactions are essential in only the short-term treatment model **(Figure 3A** in blue, **Suppl. Table 6**). Of these essential reactions, five reactions are involved in the *de novo* synthesis of thiamine diphosphate, the active form of vitamin B1 **(Figure 4** in white**).** Eight reactions were uniquely essential in the long-term treatment model **(Figure 3A** in green, **Suppl. Table 7),** notably the conversion of chorismate into 4-aminobenzoate for folate metabolism is essential **(Figure 5** in black**).**

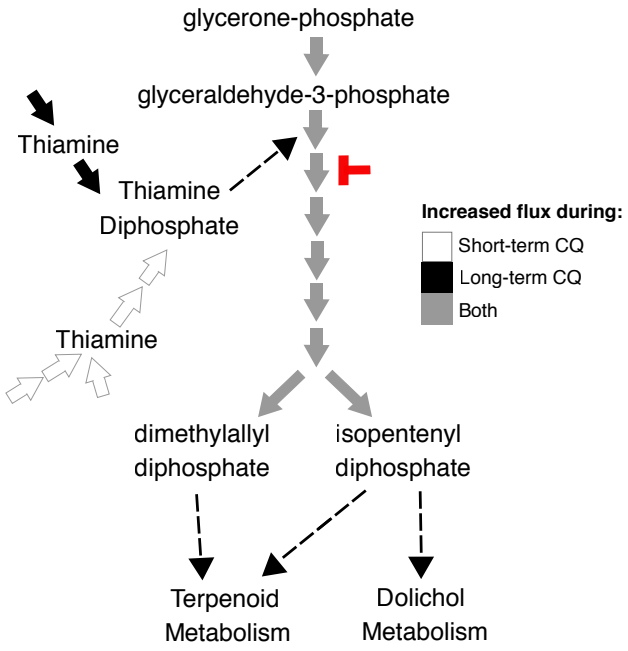

Figure 4. Increased Flux in Isoprenoids Metabolism in Response to Chloroquine. Illustration of isoprenoid metabolism reactions showing increases in flux levels in both chloroquine-treated models versus untreated models (represented in grey). 1-deoxy-D-xylulose-5-phosphate synthase utilizes thiamine diphosphate as a cofactor (marked by dotted arrow). We also predict a shift in thiamine diphosphate production, where the *de novo* synthesis pathway (shown in white) and the import pathway (shown in solid black) is used during short- and long-term treatment, respectively. Pharmacologic inhibitors target isoprenoid metabolism (fosmidomycin, indicated in red). Connectivity to other metabolic pathways are shown (dotted lines).

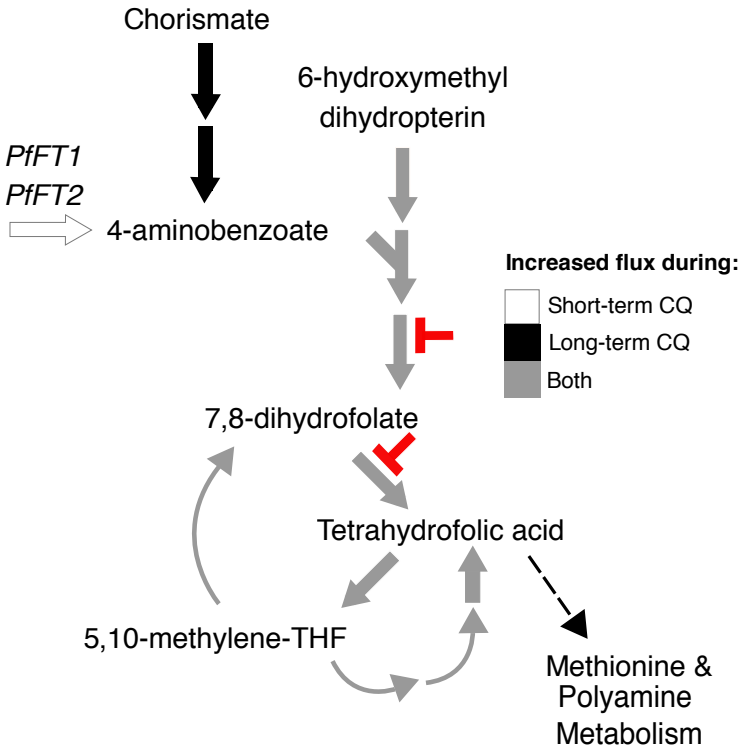

Figure 5. Increased Flux in Folate Metabolism in Response to Chloroquine. Illustration of folate metabolism reactions showing increases in flux levels in both chloroquine-treated models versus untreated models. We predict a shift in 4-aminobenzoate acquisition between short- and long-term chloroquine treatment, and elevated flux through all downstream steps of folate metabolism. Clinically available drugs target this pathway (sulfadoxine and pyrimethamine, indicated in red). Both enzymes targeted by these antimalarials (dihydropteroate synthase and dihydrofolate reductase) carry increased flux in both models of short- and long-term chloroquine treatment. Connectivity to other metabolic pathways are shown (dotted lines).

We explored why thiamine diphosphate synthesis was essential only in the short-term treatment model. *P. falciparum* has an alternate route for thiamine diphosphate production (termed 'import pathway', **Figure 4**), where thiamine is imported into the parasite's cytoplasm and phosphorylated by thiamine diphosphokinase to form thiamine diphosphate. For the untreated and long-term treatment models, only the import pathway is active. For the short-term treatment model, only the *de novo* synthesis pathway has activity. These results suggest a switch in thiamine diphosphate production in early stages of drug treatment.

Six enzymes are known to utilize thiamine diphosphate (also called thiamine pyrophosphate) as a cofactor in *P. falciparum* (44–48). Flux levels of these reactions predicted from flux balance analysis were investigated to understand thiamine diphosphate usage and essentiality. Flux balance analysis simulates steady-state flux values through the network's reactions and predicts the reactions needed to maximize the objective function, which was selected as the biomass equation; thus, this analysis predicts reactions needed for growth. Four of these thiamine diphosphate dependent enzymes (pyruvate dehydrogenase, 2-oxoglutarate dehydrogenase, 3-methyl-2-oxobutanoate dehydrogenase, and branched-chain-alpha-keto-acid dehydrogenase) are predicted to carry no flux in treated and untreated parasites. In response to drug treatment, flux changes through two thiamine diphosphate-dependent reactions: flux through the reaction catalyzed by 1-deoxy-D-xylulose phosphate synthase increases (in isoprenoids metabolism) and flux

through the reaction catalyzed by transketolase decreases (in pentose phosphate pathway). Flux of the other reactions in isoprenoids metabolism are also consistently greater in response to chloroquine treatment **(Figure 4** in grey**; Suppl. Table 8).** Compared to untreated models, short- and long-term treatment show a 62 – 83% and 24% increase in flux, respectively.

To next focus on the reactions essential in only the long-term treatment model, we explored the utilization of chorismate, a precursor of folate. During long-term chloroquine treatment, synthesis of 4-aminobenzoate from chorismate is used, rather than importing 4-aminobenzoate from the host cell **(Figure 5)**. Thus, the conversion of chorismate into 4-aminobenzoate is essential. In contrast, short-term chloroquine-treated parasites predominately rely on membrane folate transporters (PfFT1 and PfFT2) for 4-aminobenzoate **(Figure 5)**. Downstream steps in folate metabolism, including dihydropteroate synthase and dihydrofolate reductase, carry a 62.4% and 24.2% increase in flux during short- and long-term chloroquine treatment, respectively **(Figure 5** in grey; **Suppl. Table 9**).

Discussion

In this study, we used transcriptomics data to investigate metabolic shifts resulting from chloroquine treatment of resistant parasites. We performed differential expression analysis and integrated expression data into a genome-scale metabolic model to identify targetable weaknesses of chloroquine-treated resistant parasites. Using this approach, we identified metabolic pathways that, if targeted, could be developed as partner drugs for chloroquine combination therapies.

Chloroquine affects resistant parasites. Importantly, we observed a significant down-regulation of genes in response to chloroquine treatment (**Figure 2**). This suggests that chloroquine treatment continues to affect the resistant parasite, despite the parasite's resistance to the drug's cytocidal effects. This observation is consistent with growth defects observed in chloroquine-treated resistant parasites (20% and 45% inhibition after 8 and 48 hours, respectively (49)). Moreover, the effect of chloroquine is widespread and not just a function of a single gene, as evident by the numerous differentially expressed genes, and the multiple nonspecific resistance alleles (50,51). Longer exposure time exacerbates this effect, as illustrated by the increase in DEGs with the 24-hour drug treatment (**Figure 2**).

Novel proposed targets against chloroquine-resistant parasites. We propose that resistant parasites are using different metabolic pathways when in the presence of chloroquine because there are treatment-associated essential reactions. Subsystem enrichment of essentiality predictions suggests many shifts in lipid metabolism. The increased importance of phospholipids in both treatment conditions (Figure 3B) may represent the parasite's attempt to counteract the effects of chloroquine treatment. This response could occur through a number of routes: first, additional lipid species may be required to repair cellular membranes damaged by the build-up of intracellular heme during chloroquine treatment (14). Second, lipids themselves have been shown to contribute to the detoxification of heme into hemozoin (52,53). The demand for lipids for these roles may represent a targetable metabolic weakness of drug-treated chloroquine-resistant parasites.

The transport of glutathione from the extracellular environment into the cytoplasm is predicted to be essential during chloroquine treatment **(Figure 3B).** Glutathione is involved in the degradation of non-polymerized heme, in addition to being involved in managing oxidative stress in the parasite (15). Since these reactions are only essential during chloroquine treatment, this result suggests the activation of these reactions may be a direct result of drug pressure placed on the parasite and the accompanying cellular damage. This result is supported by observed correlations between chloroquine resistance and intracellular glutathione levels (54–56). The competitive inhibition of glutathione degradation by heme also supports the increased importance of glutathione accumulations to counteract chloroquine pressures (57). Thus,

glutathione is essential in combating the effects of chloroquine and can be considered another metabolic weakness of resistant parasites.

Partner drugs for chloroquine combination therapies. Folate metabolism is needed for DNA synthesis and metabolism of certain amino acids (52). Interestingly, downstream steps in folate metabolism, including dihydropteroate synthase and dihydrofolate reductase, are predicted to carry more flux during chloroquine treatment **(Figure 5)**, implying they are necessary for survival or tend to be overexpressed during treatment. This result suggests that this pathway has increased importance under chloroquine treatment and could be targeted in combination therapies. Recent clinical use of such a combination therapy supports this conclusion; chloroquine in combination with inhibitors of dihydrofolate reductase and dihydropteroate synthase (sulfadoxine-pyrimethamine) is effective against chloroquine-resistant parasites (58–60). Our results suggest that chloroquine-resistant parasites are more susceptible to these drugs than sensitive parasites and our modeling approach provides a mechanistic explanation.

Unique to our study, we predict a novel role for isoprenoids synthesis in chloroquine-resistant parasites. Under chloroquine treatment, there is increased flux through reactions in the non-mevalonate pathway for isoprenoids metabolism (**Figure 4**), the only synthesis pathway for isoprenoids in *P. falciparum* (61,62). This pathway is thiamine diphosphate-dependent and we also observed a switch in thiamine scavenging to *de novo* synthesis (**Figure 4**), highlighting the dynamic state of these pathways. Our computational analysis suggests that chloroquine-resistant parasites have increased susceptibility to non-mevalonate pathway inhibitors, such as fosmidomycin and its derivative, FR-900098 **(Figure 4)** (63). This metabolic weakness represents an ideal target since the non-mevalonate pathway is constitutively essential, with increased usage in chloroquine-treated resistant parasites (64). Fosmidomycin alone is moderately effective against chloroquine-resistant parasites (65) and there is no additivity between fosmidomycin and chloroquine *in vitro* in a pool of chloroquine-sensitive and resistant parasites (66). Thus, we propose that these parasites are even more susceptible to fosmidomycin while under chloroquine treatment. Thus, we have identified a novel combination therapy involving readily available antimalarials that may inhibit the growth of chloroquine-resistant parasites.

Conclusions

The fitness cost associated with chloroquine resistance means that once drug pressure is removed, sensitive parasites again become prominent in the population. Due to its low cost and easy access in malaria endemic countries, chloroquine use is being considered in areas where the return to sensitivity has been confirmed. However, we must be deliberate about how this drug is reinstated to avoid the rapid return of resistant parasites. Thus, we identified potential drug targets for chloroquine combination therapies, using metabolic modeling of resistant parasites under chloroquine treatment. Significantly, we identified that the combination of chloroquine with sulfadoxine-pyrimethamine or fosmidomycin may be more effective against chloroquine-resistant parasites than either drug alone; further studies will explore the use of these drugs as chloroquine resistance blockers. Additional metabolic weaknesses were found in glutathione generation and lipid synthesis during chloroquine treatment. These processes could be targeted with novel inhibitors to reduce parasite growth, thus reducing the burden of malaria infections.

References

1. WHO | World Malaria Report 2015 [Internet]. WHO. [cited 2017 Apr 12]. Available from: http://www.who.int/malaria/publications/world-malaria-report-2015/report/en/

2. Russell PK, Howson CP. Vaccines Against Malaria: Hope in a Gathering Storm [Internet]. National Academies Press (US); 1996 [cited 2017 Apr 18]. Available from: https://www.ncbi.nlm.nih.gov/books/NBK231030/

3. Chakraborty A. Emerging drug resistance in Plasmodium falciparum: A review of well-characterized drug targets for novel antimalarial chemotherapy. Asian Pac J Trop Dis. 2016 Jul 1;6(7):581–8.

4. Cowman AF, Healer J, Marapana D, Marsh K. Malaria: Biology and Disease. Cell. 2016 Oct 20;167(3):610–24.

5. Payne D. Spread of chloroquine resistance in Plasmodium falciparum. Parasitol Today Pers Ed. 1987 Aug;3(8):241–6.

6. Chou AC, Chevli R, Fitch CD. Ferriprotoporphyrin IX fulfills the criteria for identification as the chloroquine receptor of malaria parasites. Biochemistry. 1980 Apr 15;19(8):1543–9.

7. Francis SE, Sullivan DJ, Goldberg DE. Hemoglobin metabolism in the malaria parasite Plasmodium falciparum. Annu Rev Microbiol. 1997;51:97–123.

8. Goldberg DE, Slater AF, Cerami A, Henderson GB. Hemoglobin degradation in the malaria parasite Plasmodium falciparum: an ordered process in a unique organelle. Proc Natl Acad Sci U S A. 1990 Apr;87(8):2931–5.

9. Goldberg DE, Slater AF, Beavis R, Chait B, Cerami A, Henderson GB. Hemoglobin degradation in the human malaria pathogen Plasmodium falciparum: a catabolic pathway initiated by a specific aspartic protease. J Exp Med. 1991 Apr 1;173(4):961–9.

10. Fry M, Pudney M. Site of action of the antimalarial hydroxynaphthoquinone, 2-[trans-4-(4'-chlorophenyl) cyclohexyl]-3- hydroxy-1,4-naphthoquinone (566C80). Biochem Pharmacol. 1992 Apr 1;43(7):1545–53.

11. Srivastava IK, Rottenberg H, Vaidya AB. Atovaquone, a Broad Spectrum Antiparasitic Drug, Collapses Mitochondrial Membrane Potential in a Malarial Parasite. J Biol Chem. 1997 Feb 14;272(7):3961–6.

12. Francis SE, Gluzman IY, Oksman A, Knickerbocker A, Mueller R, Bryant ML, et al. Molecular characterization and inhibition of a Plasmodium falciparum aspartic hemoglobinase. EMBO J. 1994 Jan 15;13(2):306–17.

13. Sigala PA, Goldberg DE. The peculiarities and paradoxes of Plasmodium heme metabolism. Annu Rev Microbiol. 2014;68:259–78.

14. Vander Jagt DL, Hunsaker LA, Campos NM. Characterization of a hemoglobin-degrading, low molecular weight protease from Plasmodium falciparum. Mol Biochem Parasitol. 1986 Mar;18(3):389–400.

15. Zhang J, Krugliak M, Ginsburg H. The fate of ferriprotorphyrin IX in malaria infected erythrocytes in conjunction with the mode of action of antimalarial drugs. Mol Biochem Parasitol. 1999 Mar 15;99(1):129–41.

16. Loria P, Miller S, Foley M, Tilley L. Inhibition of the peroxidative degradation of haem as the basis of action of chloroquine and other quinoline antimalarials. Biochem J. 1999 Apr 15;339 (Pt 2):363–70.

17. Sullivan DJ, Gluzman IY, Russell DG, Goldberg DE. On the molecular mechanism of chloroquine's antimalarial action. Proc Natl Acad Sci U S A. 1996 Oct 15;93(21):11865–70.

18. Pagola S, Stephens PW, Bohle DS, Kosar AD, Madsen SK. The structure of malaria pigment beta-haematin. Nature. 2000 Mar 16;404(6775):307–10.

19. Fitch CD. Plasmodium falciparum in owl monkeys: drug resistance and chloroquine binding capacity. Science. 1970 Jul 17;169(3942):289–90.

20. Sanchez CP, McLean JE, Rohrbach P, Fidock DA, Stein WD, Lanzer M. Evidence for a pfcrt-Associated Chloroquine Efflux System in the Human Malarial Parasite Plasmodium falciparum. Biochemistry. 2005 Jul 1;44(29):9862–70.

21. Krogstad DJ, Gluzman IY, Kyle DE, Oduola AM, Martin SK, Milhous WK, et al. Efflux of chloroquine from Plasmodium falciparum: mechanism of chloroquine resistance. Science. 1987 Nov 27;238(4831):1283–5.

22. Fidock DA, Nomura T, Talley AK, Cooper RA, Dzekunov SM, Ferdig MT, et al. Mutations in the P. falciparum digestive vacuole transmembrane protein PfCRT and evidence for their role in chloroquine resistance. Mol Cell. 2000 Oct;6(4):861–71.

23. Roepe PD. PfCRT-mediated drug transport in malarial parasites. Biochemistry. 2011 Jan 18;50(2):163–71.

24. Martin SK, Oduola AM, Milhous WK. Reversal of chloroquine resistance in Plasmodium falciparum by verapamil. Science. 1987 Feb 20;235(4791):899–901.

25. Foote SJ, Thompson JK, Cowman AF, Kemp DJ. Amplification of the multidrug resistance gene in some chloroquine-resistant isolates of P. falciparum. Cell. 1989 Jun 16;57(6):921–30.

26. Wilson CM, Serrano AE, Wasley A, Bogenschutz MP, Shankar AH, Wirth DF. Amplification of a gene related to mammalian mdr genes in drug-resistant Plasmodium falciparum. Science. 1989 Jun 9;244(4909):1184–6.

27. Djimdé A, Doumbo OK, Cortese JF, Kayentao K, Doumbo S, Diourté Y, et al. A molecular marker for chloroquine-resistant falciparum malaria. N Engl J Med. 2001 Jan 25;344(4):257–63.

28. Wootton JC, Feng X, Ferdig MT, Cooper RA, Mu J, Baruch DI, et al. Genetic diversity and chloroquine selective sweeps in Plasmodium falciparum. Nature. 2002 Jul 18;418(6895):320–3.

29. Nagababu E, Chrest FJ, Rifkind JM. Hydrogen-peroxide-induced heme degradation in red blood cells: the protective roles of catalase and glutathione peroxidase. Biochim Biophys Acta BBA - Gen Subj. 2003 Mar 17;1620(1):211–7.

30. Kublin JG, Cortese JF, Njunju EM, Mukadam RAG, Wirima JJ, Kazembe PN, et al. Reemergence of chloroquine-sensitive Plasmodium falciparum malaria after cessation of chloroquine use in Malawi. J Infect Dis. 2003 Jun 15;187(12):1870–5.

31. Mita T, Kaneko A, Lum JK, Bwijo B, Takechi M, Zungu IL, et al. RECOVERY OF CHLOROQUINE SENSITIVITY AND LOW PREVALENCE OF THE PLASMODIUM FALCIPARUM CHLOROQUINE RESISTANCE TRANSPORTER GENE MUTATION K76T FOLLOWING THE DISCONTINUANCE OF CHLOROQUINE USE IN MALAWI. Am J Trop Med Hyg. 2003 Apr 1;68(4):413–5.

32. Laufer MK, Thesing PC, Eddington ND, Masonga R, Dzinjalamala FK, Takala SL, et al. Return of Chloroquine Antimalarial Efficacy in Malawi. N Engl J Med. 2006 Nov 9;355(19):1959–66.

33. Laufer MK, Thesing PC, Dzinjalamala FK, Nyirenda OM, Masonga R, Laurens MB, et al. A Longitudinal Trial Comparing Chloroquine as Monotherapy or in Combination with Artesunate, Azithromycin or Atovaquone-Proguanil to Treat Malaria. PLOS ONE. 2012 Aug 17;7(8):e42284.

34. Kritsiriwuthinan K, Chaotheing S, Shaw PJ, Wongsombat C, Chavalitshewinkoon-Petmitr P, Kamchonwongpaisan S. Global gene expression profiling of Plasmodium falciparum in response to the anti-malarial drug pyronaridine. Malar J. 2011 Aug 18;10:242.

35. Carey MA, Papin JA, Guler JL. Novel Plasmodium falciparum metabolic network reconstruction identifies shifts associated with clinical antimalarial resistance. BMC Genomics. 2017 Jul 19;18(1):543.

36. Ritchie ME, Phipson B, Wu D, Hu Y, Law CW, Shi W, et al. limma powers differential expression analyses for RNA-sequencing and microarray studies. Nucleic Acids Res. 2015 Apr 20;43(7):e47.

37. Wallace WJ, Houtchens RA, Maxwell JC, Caughey WS. Mechanism of autooxidation for hemoglobins and myoglobins. Promotion of superoxide production by protons and anions. J Biol Chem. 1982 May 10;257(9):4966–77.

38. Atamna H, Ginsburg H. Heme Degradation in the Presence of Glutathione A PROPOSED MECHANISM TO ACCOUNT FOR THE HIGH LEVELS OF NON-HEME IRON FOUND IN THE MEMBRANES OF HEMOGLOBINOPATHIC RED BLOOD CELLS. J Biol Chem. 1995 Oct 20;270(42):24876–83.

39. Brown SB, Hatzikonstantinou H, Herries DG. The role of peroxide in haem degradation. A study of the oxidation of ferrihaems by hydrogen peroxide. Biochem J. 1978 Sep 15;174(3):901–7.

40. Jensen PA, Papin JA. Functional integration of a metabolic network model and expression data without arbitrary thresholding. Bioinformatics. 2011 Feb 15;27(4):541–7.

41. Orth JD, Thiele I, Palsson BØ. What is flux balance analysis? Nat Biotechnol. 2010 Mar;28(3):245–8.

42. Gudmundsson S, Thiele I. Computationally efficient flux variability analysis. BMC Bioinformatics. 2010 Sep 29;11:489.

43. Becker SA, Feist AM, Mo ML, Hannum G, Palsson BØ, Herrgard MJ. Quantitative prediction of cellular metabolism with constraint-based models: the COBRA Toolbox. Nat Protoc. 2007;2(3):727–38.

44. Foth BJ, Stimmler LM, Handman E, Crabb BS, Hodder AN, McFadden GI. The malaria parasite Plasmodium falciparum has only one pyruvate dehydrogenase complex, which is located in the apicoplast. Mol Microbiol. 2005 Jan 1;55(1):39–53.

45. Oppenheim RD, Creek DJ, Macrae JI, Modrzynska KK, Pino P, Limenitakis J, et al. BCKDH: The Missing Link in Apicomplexan Mitochondrial Metabolism Is Required for Full Virulence of Toxoplasma gondii and Plasmodium berghei. PLOS Pathog. 2014 Jul 17;10(7):e1004263.

46. McMillan PJ, Stimmler LM, Foth BJ, McFadden GI, Müller S. The human malaria parasite Plasmodium falciparum possesses two distinct dihydrolipoamide dehydrogenases. Mol Microbiol. 2005 Jan;55(1):27–38.

47. Goswami AM. Computational analysis, structural modeling and ligand binding site prediction of Plasmodium falciparum 1-deoxy-d-xylulose-5-phosphate synthase. Comput Biol Chem. 2017 Feb;66:1–10.

48. Joshi S, Singh AR, Kumar A, Misra PC, Siddiqi MI, Saxena JK. Molecular cloning and characterization of Plasmodium falciparum transketolase. Mol Biochem Parasitol. 2008 Jul;160(1):32–41.

49. Yayon A, Vande Waa JA, Yayon M, Geary TG, Jensen JB. Stage-dependent effects of chloroquine on Plasmodium falciparum in vitro. J Protozool. 1983 Nov;30(4):642–7.

50. Foote SJ, Kyle DE, Martin RK, Oduola AMJ, Forsyth K, Kemp DJ, et al. Several alleles of the multidrug-resistance gene are closely linked to chloroquine resistance in Plasmodium falciparum. Nature. 1990 May;345(6272):255–8.

51. Sidhu ABS, Verdier-Pinard D, Fidock DA. Chloroquine resistance in Plasmodium falciparum malaria parasites conferred by pfcrt mutations. Science. 2002 Oct 4;298(5591):210–3.

52. Egan TJ. Haemozoin formation. Mol Biochem Parasitol. 2008 Feb 1;157(2):127–36.

53. Pisciotta JM, Coppens I, Tripathi AK, Scholl PF, Shuman J, Bajad S, et al. The role of neutral lipid nanospheres in Plasmodium falciparum haem crystallization. Biochem J. 2007 Feb 15;402(Pt 1):197–204.

54. Dubois VL, Platel DF, Pauly G, Tribouley-Duret J. Plasmodium berghei: implication of intracellular glutathione and its related enzyme in chloroquine resistance in vivo. Exp Parasitol. 1995 Aug;81(1):117–24.

55. Platel DF, Mangou F, Tribouley-Duret J. Role of glutathione in the detoxification of ferriprotoporphyrin IX in chloroquine resistant Plasmodium berghei. Mol Biochem Parasitol. 1999 Jan 25;98(2):215–23.

56. Meierjohann S, Walter RD, Müller S. Regulation of intracellular glutathione levels in erythrocytes infected with chloroquine-sensitive and chloroquine-resistant Plasmodium falciparum. Biochem J. 2002 Dec 15;368(3):761–8.

57. Famin O, Krugliak M, Ginsburg H. Kinetics of inhibition of glutathione-mediated degradation of ferriprotoporphyrin IX by antimalarial drugs. Biochem Pharmacol. 1999 Jul 1;58(1):59–68.

58. Bustos DG, Canfield CJ, Canete-Miguel E, Hutchinson DB. Atovaquone-proguanil compared with chloroquine and chloroquine-sulfadoxine-pyrimethamine for treatment of acute Plasmodium falciparum malaria in the Philippines. J Infect Dis. 1999 Jun;179(6):1587–90.

59. Hallett RL, Dunyo S, Ord R, Jawara M, Pinder M, Randall A, et al. Chloroquine/sulphadoxine-pyrimethamine for gambian children with malaria: transmission to mosquitoes of multidrug-resistant Plasmodium falciparum. PLoS Clin Trials. 2006 Jul 21;1(3):e15.

60. Menard D, Madji N, Manirakiza A, Djalle D, Koula MR, Talarmin A. Efficacy of chloroquine, amodiaquine, sulfadoxine-pyrimethamine, chloroquine-sulfadoxine-pyrimethamine combination, and amodiaquine-sulfadoxine-pyrimethamine combination in Central African children with noncomplicated malaria. Am J Trop Med Hyg. 2005 May;72(5):581–5.

61. Vial HJ, Philippot JR, Wallach DFH. A reevaluation of the status of cholesterol in erythrocytes infected by Plasmodium knowlesi and P. falciparum. Mol Biochem Parasitol. 1984 Sep 1;13(1):53–65.

62. Grellier P, Valentin A, Millerioux V, Schrevel J, Rigomier D. 3-Hydroxy-3-methylglutaryl coenzyme A reductase inhibitors lovastatin and simvastatin inhibit in vitro development of Plasmodium falciparum and Babesia divergens in human erythrocytes. Antimicrob Agents Chemother. 1994 May 1;38(5):1144–8.

63. Jomaa H, Wiesner J, Sanderbrand S, Altincicek B, Weidemeyer C, Hintz M, et al. Inhibitors of the Nonmevalonate Pathway of Isoprenoid Biosynthesis as Antimalarial Drugs. Science. 1999 Sep 3;285(5433):1573–6.

64. Ginsburg H. Progress in in silico functional genomics: the malaria Metabolic Pathways database. Trends Parasitol. 2006 Jun 1;22(6):238–40.

65. Tahar R, Basco LK. Molecular Epidemiology of Malaria in Cameroon. XXV. In Vitro Activity of Fosmidomycin and its Derivatives against Fresh Clinical Isolates of Plasmodium falciparum and Sequence Analysis of 1-Deoxy-D-Xylulose 5-Phosphate Reductoisomerase. Am J Trop Med Hyg. 2007 Aug 1;77(2):214–20.

66. Wiesner J, Henschker D, Hutchinson DB, Beck E, Jomaa H. In vitro and in vivo synergy of fosmidomycin, a novel antimalarial drug, with clindamycin. Antimicrob Agents Chemother. 2002 Sep;46(9):2889–94.

Supplemental Information

Suppl. Table 1: Reactions modified to curate the *Plasmodium falciparum* genome-scale metabolic model.

Rxn name	Rxn description	Formula	Gene-reaction association	Subsystem	Lower Bound	Upper Bound	Notes	References
HMGLB	HMGLB	hb[c] + h[c] => 36 ala_L[c] + 6 arg_L[c] + 10 asn_L[c] + 15 asp_L[c] + 3 cys_L[c] + 4 gln_L[c] + 12 glu_L[c] + 20 gly[c] + 19 his_L[c] + 36 leu_L[c] + 22 lys_L[c] + 5 met_L[c] + 15 phe_L[c] + 14 pro_L[c] + 16 ser_L[c] + 16 thr_L[c] + 3 trp_L[c] + 6 tyr_L[c] + 31 val_L[c] + pheme[fv] + h2o2[fv]	((((PF14_0076) and (PF14_0077) and (PF14_0078) and (PF14_0075) and (PF13_0133) and (PF3D7_0311700) and (PF3D7_1033800) and (PF3D7_1465700) and (PF3D7_1430200) and (PF3D7_0808200)) or ((PF11_0161) and (PF11_0162) and (PF11_0165))) and (MAL13P1_56) and (PF14_0015) and (PF14_0517) and (PFI1570c) and (PF11_0174) and (PFL2290w) and (PF13_0322) and (PF14_0439) and (PFE1360c) and (MAL8P1_140) and (PF10_0150) and (PF14_0327) and (PFF1430c) and (PFE0355c) and (PFE0370c) and (PF11_0381) and (PF14_0574))	Hemoglobin digestion	0	1000	ADD Fer; for ECs see: http://mpmp.huji.ac.il/maps/hemoglobinpolpath.html; made Plasmepsins and Falcipains OR relationship; added several Plasmepsins	MPMP; doi: 10.1073/pnas.0601876103; DOI: 10.1111/j.1365-2141.1975.tb00540.x
gthrd_heme	gthrd_heme	pheme[c] + gthrd[c] =>		Hemoglobin digestion	0	1000	Added reaction	doi: 10.1074/jbc.270.42.24876

		gthox[c] + heme_degraded[c]						
perox_heme	perox_heme	pheme[fv] + h2o2[fv] => heme_degraded[fv]		Hemoglobin digestion	0	1000	Added reaction	doi: 10.1042/bj1740893
heme_degraded_ex	heme_degraded_ex	heme_degraded[fv] =>		Exchange	0	1000	Added reaction	

1

Suppl. Table 2: Down-regulated Differentially Expressed Genes in (A) Short and (B) Long-term Chloroquine-treated Parasites.

Suppl. Table 2A. Down-regulated genes in short-term chloroquine-treated condition

Gene ID	Gene Name	Fold Change
MAL13P1.252	Conserved Plasmodium protein, Unknown Function	0.191
PF14_0010	GBPH protein	0.200
PFF1080w	Conserved Plasmodium protein, Unknown Function	0.205
PFF1410c	Nicotinate phosphoribosyltransferase	0.215
MAL13P1.306	Conserved Plasmodium protein, Unknown Function	0.221
PFL0365c	LIMP protein	0.235
PFE0015c	Rifin	0.237
PFF0155w	Mitochondrial chaperone BCS1	0.243
PF07_0087	Conserved Plasmodium protein, Unknown Function	0.263
PF10_0222	CDGSH iron-sulfur domain-containing protein	0.269
PF13_0010	GBPH2 protein	0.273
PFL1035w	Conserved Plasmodium protein, Unknown Function	0.281
PF14_0317	Signal peptidase complex subunit SPC1	0.294
PF11_0159	Conserved Plasmodium protein, Unknown Function	0.294
PF10_0265	Conserved Plasmodium protein, Unknown Function	0.298
PF10_0159	GBP130 protein	0.302
PFI0220w	Prefoldin subunit 4	0.314
PF10_0041	U5 small nuclear ribonucleoprotein component	0.315
MAL7P1.75	Mitochondrial ATP synthase epsilon subunit	0.332
PF13_0141	L-lactate dehydrogenase	0.350
MAL8P1.3	Plasmodium exported protein (hyp9), Unknown Function	0.365
PFL2050w	Farnesyltransferase alpha subunit	0.365
PFF1310c	Conserved Plasmodium protein, Unknown Function	0.367
PFF0700c	60S ribosomal protein L19	0.367
PFA0310c	Calcium-transporting ATPase	0.375
PF10_0264	40S ribosomal protein S2	0.376
PF10_0092	Metalloprotease	0.377
PF11_0351	Heat shock protein 70	0.379
PFF0335c	VFT protein	0.381
PFF0030c	Erythrocyte membrane protein 1 (PfEMP1), exon 2	0.382
PFF0435w	Ornithine aminotransferase	0.382
PFA0540c	Conserved Plasmodium protein, Unknown Function	0.386
PF14_0394	Conserved Plasmodium protein, Unknown Function	0.387
PFL1140w	Vacuolar iron transporter	0.391
PFL0840c	Conserved Plasmodium protein, Unknown Function	0.391
PF13_0063	26S protease regulatory subunit 7	0.394
PF14_0680	Conserved Plasmodium protein, Unknown Function	0.398

PFE0050w	Conserved Plasmodium protein, Unknown Function	0.399
PFI1270w	Conserved Plasmodium protein, Unknown Function	0.401
PFI1105w	Phosphoglycerate kinase	0.409
PF14_0581	Apicoplast ribosomal protein S10	0.410
MAL8P1.83	Eukaryotic translation initiation factor 3 subunit G	0.412
MAL13P1.250	Conserved Plasmodium protein, Unknown Function	0.412
PFI1090w	S-adenosylmethionine synthetase	0.413
PFI1695c	U2 small nuclear ribonucleoprotein B"	0.413
PFA0660w	Heat shock protein 40, type II	0.414
PFE1100w	Conserved Plasmodium protein, Unknown Function	0.418
PF13_0252	Nucleoside transporter 1	0.419
PF11_0167	Palmitoyltransferase DHHC9	0.433
PF10_0144	Prohibitin	0.433
PFL1420w	Macrophage migration inhibitory factor	0.434
PF10_0024	Plasmodium exported protein (hyp2), Unknown Function	0.439
PF10_0063	DNA/RNA-binding protein Alba 3	0.440
PFC0520w	26S proteasome regulatory subunit RPN12	0.442
PFF0950w	Conserved Plasmodium protein, Unknown Function	0.444
MAL13P1.76	General transcription factor IIH subunit 2	0.445
PFC0350c	T-complex protein 1 eta subunit	0.447
PF14_0331	Cytochrome c oxidase assembly protein COX15	0.448
PF14_0387	Major facilitator superfamily domain-containing protein	0.448
PF14_0275	Conserved Plasmodium protein, Unknown Function	0.451
PF11_0224	Exported protein 1	0.452
PFE0285c	Small ubiquitin-related modifier	0.454
PFL0175c	Threonylcarbamoyl-AMP synthase	0.455
PFE1050w	Adenosylhomocysteinase	0.455
PF14_0448	40S ribosomal protein S5	0.458
PF10_0240	RAP protein	0.459
PF07_0043	60S ribosomal protein L34	0.460
PF14_0167	Prefoldin subunit 2	0.462
PFC0400w	60S acidic ribosomal protein P2	0.463
MAL8P1.50	Conserved Plasmodium protein, Unknown Function	0.464
PFL2515c	Conserved Plasmodium protein, Unknown Function	0.466
PF14_0442	Conserved Plasmodium protein, Unknown Function	0.470
MAL8P1.33	GTP-binding protein	0.472
PF10_0187	60S ribosomal protein L30e	0.473
PFB0840w	Replication factor C subunit 2	0.475
MAL7P1.94	Prefoldin subunit 3	0.476
MAL8P1.145	Mitogen-activated protein kinase organizer 1	0.477
MAL8P1.128	Proteasome subunit alpha type-6	0.478
PF10_0289	Adenosine deaminase	0.478

PFI1045w	Conserved Plasmodium protein, Unknown Function	0.480
PFL1630c	Conserved Plasmodium protein, Unknown Function	0.480
PF08_0099	Acyl-CoA binding protein	0.481
PF13_0080	Telomerase reverse transcriptase	0.484
PFE0945c	Secreted ookinete protein	0.487
PF08_0087	Karyopherin alpha	0.490
MAL13P1.88	Conserved Plasmodium protein, Unknown Function	0.490
PF14_0266	Conserved Plasmodium protein, Unknown Function	0.491
PF13_0045	40S ribosomal protein S27	0.492
PFL2465c	Thymidylate kinase	0.493
PFI1545c	Proteasome beta subunit type-6	0.494
PF07_0065	Cation diffusion facilitator family protein	0.494
MAL13P1.153	Ribonuclease P protein subunit RPR2	0.498
PF11_0461	Ras-related protein Rab-6	0.499

Suppl. Table 2B. Down-regulated genes in long-term chloroquine-treated condition

Gene ID	Gene Name	Fold Change
PF14_0010	GBPH protein	0.169
PF10_0041	U5 small nuclear ribonucleoprotein component	0.172
MAL13P1.252	Conserved Plasmodium protein, Unknown Function	0.184
PF13_0010	GBPH2 protein	0.201
PFE0015c	Rifin	0.220
MAL13P1.306	Conserved Plasmodium protein, Unknown Function	0.221
PFF1410c	Nicotinate phosphoribosyltransferase	0.224
PFL0365c	LIMP protein	0.263
PF07_0087	Conserved Plasmodium protein, Unknown Function	0.270
PF11_0159	Conserved Plasmodium protein, Unknown Function	0.281
PF10_0159	GBP130 protein	0.286
PF11_0167	Palmitoyltransferase DHHC9	0.294
PF11_0351	Heat shock protein 70	0.299
PFL2050w	Farnesyltransferase alpha subunit	0.307
PFC0400w	60S acidic ribosomal protein P2	0.310
PF10_0222	CDGSH iron-sulfur domain-containing protein	0.311
PFA0310c	Calcium-transporting ATPase	0.312
MAL13P1.88	Conserved Plasmodium protein, Unknown Function	0.321
PF10_0024	Plasmodium exported protein (hyp2), Unknown Function	0.321
PF13_0141	L-lactate dehydrogenase	0.323
PF14_0394	Conserved Plasmodium protein, Unknown Function	0.328
MAL7P1.75	Mitochondrial ATP synthase epsilon subunit	0.329
PF14_0387	Major facilitator superfamily domain-containing protein	0.330
PF10_0092	Metalloprotease	0.331

PF11_0224	Circumsporozoite-related antigen	0.334
PF11_0338	Aquaglyceroporin	0.336
MAL8P1.50	Conserved Plasmodium protein, Unknown Function	0.337
PFF1310c	Conserved Plasmodium protein, Unknown Function	0.338
PF11_0495	Conserved Plasmodium protein, Unknown Function	0.340
PF08_0087	Karyopherin alpha	0.342
PFA0660w	Heat shock protein 40, type II	0.345
PFA0435w	Conserved Plasmodium protein, Unknown Function	0.345
PFI0220w	Prefoldin subunit 4	0.346
PFE1100w	Conserved Plasmodium protein, Unknown Function	0.347
PFE1050w	Adenosylhomocysteinase	0.350
PF10_0265	Conserved Plasmodium protein, Unknown Function	0.351
PFL0840c	Conserved Plasmodium protein, Unknown Function	0.352
PF10_0264	40S ribosomal protein S2	0.357
PFF0030c	Erythrocyte membrane protein 1 (PfEMP1), exon 2	0.359
PFF0700c	60S ribosomal protein L19	0.361
PFF0435w	Ornithine aminotransferase	0.365
PFL2260w	Conserved Plasmodium protein, Unknown Function	0.367
PFD0365c	Conserved Plasmodium protein, Unknown Function	0.367
MAL8P1.83	Eukaryotic translation initiation factor 3 subunit G	0.368
PFA0540c	Conserved Plasmodium protein, Unknown Function	0.368
PF14_0275	Conserved Plasmodium protein, Unknown Function	0.368
PFL1445w	TBC domain-containing protein	0.375
PF14_0442	Conserved Plasmodium protein, Unknown Function	0.375
MAL13P1.76	General transcription factor IIH subunit 2	0.376
PFE0050w	Plasmodium exported protein, unknown function	0.377
PF14_0522	Conserved Plasmodium protein, Unknown Function	0.377
PFB0840w	Replication factor C subunit 2	0.378
PF13_0063	26S protease regulatory subunit 7	0.382
MAL13P1.250	Conserved Plasmodium protein, Unknown Function	0.384
PFL0850w	Anaphase-promoting complex subunit 10	0.386
PF10_0240	RAP protein	0.387
MAL7P1.174	Lysine-rich membrane-associated PHISTb protein	0.388
PF10_0141	MO15-related protein kinase	0.392
PFI0190w	60S ribosomal protein L32	0.392
PF13_0219	Nucleolar complex protein 2	0.392
PFI1545c	Proteasome beta subunit type-6	0.394
PFE1020w	U6 snRNA-associated Sm-like protein LSm2	0.398
PF14_0581	Apicoplast ribosomal protein S10	0.404
PF10_0144	Prohibitin	0.409
PFE0030c	Stevor	0.409
PF07_0043	60S ribosomal protein L34	0.412

PFL0175c	Threonylcarbamoyl-AMP synthase	0.414
PF11_0290	Conserved Plasmodium protein, Unknown Function	0.418
PFE0285c	Small ubiquitin-related modifier	0.421
PFI1695c	U2 small nuclear ribonucleoprotein B"	0.422
MAL13P1.261	Conserved Plasmodium protein, Unknown Function	0.422
PF10_0016	Acyl-CoA binding protein, isoform 2, ACBP2	0.424
PF10_0289	Adenosine deaminase	0.429
PF13_0252	Cytochrome c oxidase copper chaperone	0.432
PFC0520w	26S proteasome regulatory subunit RPN12	0.440
PF13_0021	Small heat shock protein	0.444
MAL13P1.490	Stevor	0.444
PF10_0187	60S ribosomal protein L30e	0.444
PFI1105w	Phosphoglycerate kinase	0.445
PF14_0555	Conserved Plasmodium protein, Unknown Function	0.446
PF11_0461	Ras-related protein Rab-6	0.448
PF14_0331	Cytochrome c oxidase assembly protein COX15	0.448
PFF1515c	Erythrocyte membrane protein 1 (PfEMP1)	0.449
PF14_0424	Shikimate dehydrogenase	0.450
PF10_0063	DNA/RNA-binding protein Alba 3	0.450
MAL8P1.125	Tyrosine--tRNA ligase	0.451
MAL13P1.160	Conserved Plasmodium protein, Unknown Function	0.454
MAL13P1.182	RanBPM and CLTH-like protein	0.458
PFL2485c	Tryptophan--tRNA ligase	0.461
PF08_0099	Acyl-CoA binding protein	0.463
MAL13P1.142	WD repeat-containing protein	0.463
PF10_0320	Leucine-rich repeat protein 8, LRR8	0.464
PFE0905w	RAP protein	0.464
PFL2540w	Plasmodium exported protein (PHISTb), unknown function	0.464
PFD0540c	Conserved Plasmodium protein, Unknown Function	0.465
MAL8P1.145	Mitogen-activated protein kinase organizer 1	0.466
PFD0890w	Conserved Plasmodium protein, Unknown Function	0.466
PF14_0228	Conserved Plasmodium protein, Unknown Function	0.466
PF08_0039	60S ribosomal protein L22	0.468
PFF0950w	Conserved Plasmodium protein, Unknown Function	0.469
PF13_0117	TBC domain protein	0.469
PF14_0732	Lysine-rich membrane-associated PHISTb protein	0.470
PF10_0312	Conserved Plasmodium protein, Unknown Function	0.470
PFE0410w	Triose phosphate transporter	0.471
PFE1450c	Thioredoxin-like protein	0.472
PF11_0183	GTP-binding nuclear protein RAN/TC4	0.473
MAL7P1.57	Rifin	0.473

PFE0150c	4-diphosphocytidyl-2-C-methyl-D-erythritol kinase	0.474
PFE0940c	Secreted ookinete protein	0.477
PF07_0065	Cation diffusion facilitator family protein	0.478
PF10_0131	Conserved Plasmodium protein, Unknown Function	0.478
MAL7P1.152	Conserved Plasmodium protein, Unknown Function	0.478
PF10_0047	RNA-binding protein	0.480
PFF1570w	Rifin	0.481
PFD0795w	Histone acetyltransferase	0.482
MAL13P1.93	Nucleolar complex protein 4	0.482
PFD0480w	Peptide chain release factor 2	0.482
PF07_0053	Conserved Plasmodium protein, Unknown Function	0.483
PF14_0266	Conserved Plasmodium protein, Unknown Function	0.484
PF10_0018	Exported lipase 1	0.484
MAL13P1.153	Ribonuclease P protein subunit RPR2	0.484
PFB0865w	Small nuclear ribonucleoprotein Sm D2	0.485
PF10_0271	Centrin-3	0.489
PFF1020c	Conserved Plasmodium protein, Unknown Function	0.490
PF13_0316	40S ribosomal protein S15	0.491
PF08_0010	Conserved Plasmodium protein, Unknown Function	0.491
PFE1285w	Inner membrane complex protein 1g	0.492
PF11_0052	Syntaxin, Qa-SNARE family	0.495
PF11_0056	WD repeat-containing protein	0.495
PFC0350c	T-complex protein 1 subunit eta	0.496
PF10_0046	E3 ubiquitin-protein ligase	0.497
PF13_0107	Conserved Plasmodium protein, Unknown Function	0.498
PF11_0350	Conserved Plasmodium protein, Unknown Function	0.498
PF14_0645	Conserved Plasmodium protein, Unknown Function	0.498
PF14_0448	40S ribosomal protein S5	0.499
PFD1140w	Plasmodium exported protein (PHISTc), unknown function	0.499
PFD0460c	Conserved Plasmodium protein, Unknown Function	0.500
PFL1140w	Vacuolar iron transporter	0.500

The gene IDs, corresponding gene names, and fold changes of significantly down-regulated genes in response to chloroquine treatment.

Suppl. Table 3: Up-regulated Differentially Expressed Genes in (A) Short and (B) Long-term Chloroquine-treated Parasites.

Suppl. Table 3A. Up-regulated genes in short-term chloroquine-treated condition

Gene ID	Gene Name	Fold Change
PF11_0223	Conserved Plasmodium protein, Unknown Function	2.532
PFI1550c	adenylate kinase-like protein 2	2.242

PF10_0050	Conserved Plasmodium protein, Unknown Function	2.060
PF11_0516	Stevor	2.034

Suppl. Table 3B. Up-regulated genes in long-term chloroquine-treated condition

Gene ID	Gene Name	Fold Change
MAL13P1.294	GTP-binding protein	4.730
PFB0106c	EMP1-trafficking protein	2.409
MAL7P1.141	Conserved Plasmodium protein, Unknown Function	2.388
PFL1090w	Glideosome-associated protein 45	2.373
PFL1040w	protein TSSC1	2.351
PFI0270w	Conserved Plasmodium protein, Unknown Function	2.315
PF14_0044	Conserved Plasmodium protein, Unknown Function	2.308
PFD0120w	Rifin	2.274
PFD0465w	Chaperone DnaJ protein	2.230
PFE1535w	Conserved Plasmodium protein, Unknown Function	2.225
PF13_0276	Membrane associated histidine-rich protein	2.205
MAL8P1_99	GTPase	2.186
PF11_0328	Conserved Plasmodium protein, Unknown Function	2.168
PFL1000c	Conserved Plasmodium protein, Unknown Function	2.127
PF11_0036	Phosphopantothenate--cysteine ligase	2.113
PF14_0238	Conserved Plasmodium protein, Unknown Function	2.101
PFF0485c	Palmitoyltransferase DHHC2	2.096
PF11_0113	Mitochondrial ribosomal protein L11 precursor	2.069
PF11_0002	Conserved Plasmodium protein, Unknown Function	2.067
PF08_0035	Conserved Plasmodium protein, Unknown Function	2.066
PFI0940c	PPPDE peptidase	2.058
PFI1095w	Conserved Plasmodium protein, Unknown Function	2.054
MAL7P1.161	Dynein light chain	2.051
PF10_0050	Conserved Plasmodium protein, Unknown Function	2.047
PFC0176c	Phosphatidylethanolamine-binding protein	2.039
PF11_0204	Conserved Plasmodium protein, Unknown Function	2.036
PFD0705c	Acylated pleckstrin-homology domain-containing protein	2.010
PFL1025c	Conserved Plasmodium protein, Unknown Function	2.005

The gene IDs, corresponding gene names, and fold changes of significantly up-regulated genes in response to chloroquine treatment.

Suppl. Table 4: Significant Down Regulation of Metabolic Genes Arising from Chloroquine Treatment.

Suppl. Table 4A: Metabolic Differentially Expressed Genes Common to Long and Short-term Treated Conditions

Gene ID	Gene Name	Subsystem
PFF1410c	nicotinate phosphoribosyltransferase	Nicotinate & Nicotinamide Metabolism

MAL7P1_75	mitochondrial ATP synthase F1, epsilon subunit	Mitochondria Transport
PF13_0141	L-lactate dehydrogenase	Glycolysis
PFF0435w	ornithine aminotransferase	Arg & Pro Metabolism
PFI1105w	phosphoglycerate kinase	Glycolysis
PF13_0252	nucleoside transporter 1	Base Transport
PF14_0331	cytochrome c oxidase assembly protein COX15	Mitochondrial Electron Flow
PFE1050w	Adenosylhomocysteinase	Met & Polyamine Metabolism
PF10_0289	adenosine deaminase	Met & Polyamine Metabolism, Purine Metabolism

Suppl. Table 4B: Metabolic Differentially Expressed Genes Unique to Short-term Treated Condition

Gene ID	Gene Name	Subsystem
PFI1090w	S-adenosylmethionine synthetase	Met & Polyamine Metabolism
PFL2465c	thymidylate kinase	Pyrimidine Metabolism

The gene IDs, corresponding gene names, and metabolic subsystems of genes with significant expression changes in response to chloroquine treatment.

Suppl. Table 4C: Metabolic Differentially Expressed Genes Unique to Long-term Treated Condition

Gene ID	Gene Name	Subsystem
PF11_0338	Aquaglyceroporin	Transport
MAL8P1_125	tyrosine--tRNA ligase	Phe & Tyr Metabolism
PFL2485c	tryptophan--tRNA ligase	Trp Metabolism, tRNA Synthesis
PFE0410w	triose phosphate transporter	Apicoplast Transport
PFE0150c	4-diphosphocytidyl-2-C-methyl-D-erythritol kinase	Isoprenoids Metabolism
PF11_0036	Phosphopantothenate-cysteine ligase	CoA Biosynthesis

The gene IDs, corresponding gene names, and metabolic subsystems of genes with significant expression changes in response to chloroquine treatment.

Suppl. Table 5. Reactions Essential in only Chloroquine-Treated Models.

Reaction ID	Enzyme Name	Reaction Formula	Subsystem
EX_gthrd(e)	--	gthrd[e] <=>	Exchange
EX_nac(e)	--	nac[e] <=>	Exchange

lipid4	--	cdpdag[c] <=> cdpdddecg[c] + cdpdhdec9eg[c] + cdpdhdecg[c] + cdpdodec11eg[c] + cdpdodecg[c] + cdpdtdec7eg[c] + cdpdtdecg[c]	Lipids
DAGK120	Diacylglycerol Kinase	12dgr120[c] + atp[c] => adp[c] + h[c] + pa120[c]	Phosphatidyletanolamine & Phosphatidylserine Metabolism; Utilization Phospholipids
DAGK140	Diacylglycerol Kinase	12dgr140[c] + atp[c] => adp[c] + h[c] + pa140[c]	Phosphatidyletanolamine & Phosphatidylserine Metabolism; Utilization Phospholipids
DAGK141	Diacylglycerol Kinase	12dgr141[c] + atp[c] => adp[c] + h[c] + pa141[c]	Phosphatidyletanolamine & Phosphatidylserine Metabolism; Utilization Phospholipids
DAGK160	Diacylglycerol Kinase	12dgr160[c] + atp[c] => adp[c] + h[c] + pa160[c]	Phosphatidyletanolamine & Phosphatidylserine Metabolism; Utilization Phospholipids
DAGK161	Diacylglycerol Kinase	12dgr161[c] + atp[c] => adp[c] + h[c] + pa161[c]	Phosphatidyletanolamine & Phosphatidylserine Metabolism; Utilization Phospholipids
DAGK180	Diacylglycerol Kinase	12dgr180[c] + atp[c] => adp[c] + h[c] + pa180[c]	Phosphatidyletanolamine & Phosphatidylserine Metabolism; Utilization Phospholipids
DAGK181	Diacylglycerol Kinase	12dgr181[c] + atp[c] => adp[c] + h[c] + pa181[c]	Phosphatidyletanolamine & Phosphatidylserine Metabolism; Utilization Phospholipids
DASYN120	Phosphatidate Cytidylyltransferase	ctp[c] + h[c] + pa120[c] => cdpdddecg[c] + ppi[c]	Phosphatidyletanolamine & Phosphatidylserine Metabolism
DASYN140	Phosphatidate Cytidylyltransferase	ctp[c] + h[c] + pa140[c] => cdpdtdecg[c] + ppi[c]	Phosphatidyletanolamine &

			Phosphatidylserine Metabolism
DASYN141	Phosphatidate Cytidylyltransferase	ctp[c] + h[c] + pa141[c] => cdpdtdec7eg[c] + ppi[c]	Phosphatidyletanolamine & Phosphatidylserine Metabolism
DASYN160	Phosphatidate Cytidylyltransferase	ctp[c] + h[c] + pa160[c] => cdpdhdecg[c] + ppi[c]	Phosphatidyletanolamine & Phosphatidylserine Metabolism
DASYN161	Phosphatidate Cytidylyltransferase	ctp[c] + h[c] + pa161[c] => cdpdhdec9eg[c] + ppi[c]	Phosphatidyletanolamine & Phosphatidylserine Metabolism
DASYN180	Phosphatidate Cytidylyltransferase	ctp[c] + h[c] + pa180[c] => cdpdodecg[c] + ppi[c]	Phosphatidyletanolamine & Phosphatidylserine Metabolism
DASYN181	Phosphatidate Cytidylyltransferase	ctp[c] + h[c] + pa181[c] => cdpdodec11eg[c] + ppi[c]	Phosphatidyletanolamine & Phosphatidylserine Metabolism
PINOS	CDP-diacylglycerol-inositol 3-phosphatidyltransferase	0.01 cdpdag[c] + inost[c] => cmp[c] + h[c] + 0.01 ptd1ino[c]	Inositol Phosphate Metabolism
NACUP	--	nac[e] => nac[c]	Cofactor Transport
trna_gln	--	trnagln[c] <=>	AminoAcids tRNA; Exchange
trna_glu	--	trnaglu[c] <=>	AminoAcids tRNA; Exchange
GLNTRS	Glutamine--tRNA Ligase	atp[c] + gln_L[c] + trnagln[c] => amp[c] + ppi[c] + glntrna[c]	Glu Metabolism; AminoAcids tRNA
GLUTRS	Glutamate--tRNA Ligase	atp[c] + glu_L[c] + trnaglu[c] => amp[c] + glutrna[c] + ppi[c]	Glu Metabolism; AminoAcids tRNA
GPDDA4	Glycerophosphodiester Phosphodiesterase	g3pg[c] + h2o[c] => glyc3p[c] + glyc[c] + h[c]	Phosphatidylcholine Metabolism; Phosphatidyletanolamine & Phosphatidylserine Metabolism
GTHRDti	--	gthrd[e] => gthrd[c]	Transport; Redox Metabolism
GHMT2r	Serine Hydroxymethyltransferase	ser_L[c] + thf[c] <=> gly[c] + h2o[c] + mlthf[c]	Pyrimidine Metabolism; Gly Ser

			Metabolism; Folate Biosynthesis
GAT_c	Diacylglycerol O-Acyltransferase	dag[c] + acoa[c] => coa[c] + tag[c]	Lipid Production
CHLPCTD	Choline-phosphate Cytidylyltransferase	cholp[c] + ctp[c] + h[c] -> cdpchol[c] + ppi[c]	Phosphatidylcholine Metabolism
SMPD3l_host	Sphingomyelin Phosphodiesterase	h2o[c] + sphmyln_host[c] -> cholp[c] + crm[c] + h[c]	Sphingomyelin and Ceramide Metabolism
SM_ex	--	sphmyln[e] <=>	Exchange
SM_host	--	sphmyln[e] -> sphmyln_host[c]	Extracellular Transport
Hfv	--	pheme[fv] -> pheme[c]	Hemoglobin Digestion

The reaction IDs, corresponding enzyme names, reaction formulas, and metabolic subsystems of essential reactions common to chloroquine-treated condition models constructed with varying growth thresholds (30 – 80%).

Suppl. Table 6. Reactions Essential in only the Short-Term Treatment Condition.

Reaction ID	Enzyme Name	Reaction Formula	Subsystem
HMPK1	Hydroxymethylpyrimidine Kinase	4ahmmp[c] + atp[c] => 4ampm[c] + adp[c] + h[c]	Thiamine Metabolism
PMPK	Phosphomethylpyrimidine Kinase	4ampm[c] + atp[c] => 2mahmp[c] + adp[c]	Thiamine Metabolism
TMPK	Thiamine-Phosphate Kinase	atp[c] + thmmp[c] => adp[c] + thmpp[c]	Thiamine Metabolism
TMPPP	Thiamine-Phosphate Diphosphorylase	2mahmp[c] + 4mpetz[c] + h[c] => ppi[c] + thmmp[c]	Thiamine Metabolism
4HBAtmt	--	4hba[m] <=> 4hba[c]	Mitochondrial Transport
ALALtmt	--	ala_L[m] <=> ala_L[c]	Mitochondrial Transport
CYSLtmt	--	cys_L[m] <=> cys_L[c]	Mitochondrial Transport
DXYL5Ptmt	--	dxyl5p[m] <=> dxyl5p[c]	Mitochondrial Transport
EX_4ahmmp	--	4ahmmp[e] <=>	Exchange
4AHMMPtr	--	4ahmmp[e] <=> 4ahmmp[c]	Transport
DXYL5Ptap	--	dxyl5p[ap] <=> dxyl5p[c]	Apicoplast Transport
4MHETZtmt	--	4mhetz[m] <=> 4mhetz[c]	Mitochondrial Transport
HETZK	Hydroxyethylthiazole Kinase	4mhetz[c] + atp[c] => 4mpetz[c] + adp[c] + h[c]	Thiamine Metabolism
EX_4HBA	--	4hba[c] =>	Exchange

The reaction IDs, corresponding enzyme names, reaction formulas, and metabolic subsystems of essential reactions unique to the short-term chloroquine-treated condition models (30 – 80% growth thresholds).

Suppl. Table 7. Reactions Essential in only the Long-Term Treatment Condition.

Reaction ID	Enzyme	Reaction Formula	Subsystem
PGMT_2	Phosphoglucomutase	r1p[c] <=> r5p[c]	Pentose Phosphate Cycle; Glycolysis
ADPtap	--	adp[ap] <=> adp[c]	Apicoplast Transport
ATPtap	--	atp[ap] <=> atp[c]	Apicoplast Transport
PYK	Pyruvate Kinase	adp[c] + h[c] + pep[c] => atp[c] + pyr[c]	Glycolysis; Pyruvate Metabolism; Isoprenoids Metabolism; Fatty Acid Synthesis
ADCL	Aminodeoxychorismate Lyase	4adcho[c] => 4abz[c] + h[c] + pyr[c]	Shikimate Biosynthesis; Folate Biosynthesis
ADCS	para-Aminobenzoic Acid Synthetase	chor[c] + gln_L[c] => 4adcho[c] + glu_L[c]	Folate Biosynthesis; Shikimate Biosynthesis

The reaction IDs, corresponding enzyme names, reaction formulas, and metabolic subsystems of essential reactions unique to the long-term chloroquine-treated condition models (30 – 80% growth thresholds).

Suppl. Table 8. Flux Values for Isoprenoid Metabolism Reactions in the Chloroquine-treated and Untreated Models.

Reactions	Corresponding Enzymes	Short-term CQ	Short-term No CQ	Long-term CQ	Long-term No CQ
TPI	Triose-phosphate isomerase	0.013284	0	0.033163	0
TPI[ap]	Triose-phosphate isomerase [apicoplast]	0.059777	0.032710	0.053061	0.042733
PYK[ap]	Pyruvate kinase [apicoplast]	0.059777	520.1499	0.053061	626.768
CDPMEK[ap]	4-(cytidine 5'-diphospho)-2-C-methyl-D-erythritol kinase [apicoplast]	0.053135	0.032710	0.053061	0.042733
DMPPS[ap]	4-hydroxy-3-methylbut-2-enyl diphosphate reductase [apicoplast]	0.006642	0.004089	0.006633	0.005342
DXPRIi[ap]	1-deoxy-D-xylulose-5-phosphate	0.053135	0.032710	0.053061	0.042733

	reductoisomerase [apicoplast]				
DXPS[ap]	1-deoxy-D-xylulose-5-phosphate synthase [apicoplast]	0.059777	0.032710	0.053061	0.042733
IPDPS[ap]	4-hydroxy-3-methylbut-2-enyl diphosphate reductase [apicoplast]	0.046493	0.028621	0.046428	0.037392
MECDPDH2[ap]	2C-methyl-D-erythritol 2,4 cyclodiphosphate dehydratase [apicoplast]	0.053135	0.032710	0.053061	0.042733
MECDPS[ap]	2-C-methyl-D-erythritol 2,4-cyclodiphosphate synthase [apicoplast]	0.053135	0.032710	0.053061	0.042733
MEPCT[ap]	2-C-methyl-D-erythritol 4-phosphate cytidylyltransferase [apicoplast]	0.053135	0.032710	0.053061	0.042733
PYK	Pyruvate kinase	999.9601	0	999.8939	0
PYK[ap]2	Pyruvate kinase [apicoplast]	0	0	0	0

Results represent median flux values across condition models constructed with varying growth thresholds (30 - 80%). Bolded reactions are represented in Figure 4.

Suppl. Table 9. Flux Values for Folate Metabolism Reactions in the Chloroquine-treated and Untreated Models.

Reactions	Corresponding Enzymes	Short-term CQ	Short-term No CQ	Long-term CQ	Long-term No CQ
FMETTRS	Methionyl-tRNA formyltransferase	0.297843	0.183353	0.297428	0.239536
AKP1	Alkaline phosphatase	0.059777	0.032710	0.053061	0.042733
DHFR	Dihydrofolate reductase	0.830357	0.689333	0.829198	0.667803
DHFS	Dihydrofolate synthase	0.019926	0.016542	0.019898	0.016025
DHPS2	Dihydropteroate synthase	0.019926	0.016542	0.019898	0.016025
GTPCI	GTP cyclohydrolase I	0	0	0	0
HPPK2	2-amino-4-hydroxy-6-hydroxymethyldihydropteridine diphosphokinase	0.019926	0.016542	0.019898	0.016025

MTHFC	Methenyltetrahydrofolate cyclohydrolase	0.304485	0.252773	0.30406	0.244878
MTHFD	Methylenetetrahydrofolate dehydrogenase (NADP+)	0.304485	0.252773	0.30406	0.244878
PTHPS	6-pyruvoyltetrahydropterin synthase	0	0	0	0
THFGLUS	Tetrahydrofolate synthase	0	0	0	0
TMDS	Thymidylate synthase	0.810432	0.672792	0.8093	0.651778
PTHPS2	6-pyruvoyltetrahydropterin synthase	0	0	0	0
ADCL	4-aminobenzoate synthase	0	0	0.019898	0
ADCS	4-amino-4-deoxychorismate synthase	0	0	0.019898	0
GHMT2r	Glycine hydroxymethyltransferase	1.121559	0.931078	1.119993	0
GHMT2r_m	Glycine hydroxymethyltransferase [mitochondria]	0	0	0	0
GHMT2r_ap	Glycine hydroxymethyltransferase [apicoplast]	0	0	0	0
pABAt	Folate transporter 1 & 2	0.019926	0.012266	0	0.016025

Results represent median flux values across condition models constructed with varying growth thresholds (30 - 80%). Bolded reactions are represented in Figure 5.

Ethics approval and consent to participate

Not applicable.

Consent for publication

Not applicable.

Availability of data and materials:

The publically available dataset analyzed during the current study are available on the NCBI's Gene Expression Omnibus, GSE31109. Additionally, our curated model and code are available on GitHub, at https://github.com/anauntaroiu/Chloroquine-Project.

Competing interests

The authors declare that they have no competing interests.

Funding

The study was financed by the National Institute of Allergy and Infectious Disease (R21AI119881 - JG and JP), an institutional training grant (T32GM008136 - MC), and the Arnold and Mabel Beckman Foundation (via the Beckman Scholars program - AU).

Authors' contributions

AU and MC designed the study. AU curated the model and performed statistical and network analyses. AU and MC interpreted the data and analyses. AU wrote the manuscript. MC, JG, and JP edited the manuscript. JG and JP provided resources. All authors read and approved the final manuscript.

Acknowledgements

We thank the members of the Guler and Papin labs for their thoughtful feedback and the openCobra community for software development integral to this work.